CrossMark

MR-guided microwave ablation in hepatic tumours: initial results in clinical routine

Rüdiger Hoffmann[1] · Hansjörg Rempp[1] · David-Emanuel Keßler[1] · Jakob Weiß[1] ·
Philippe L. Pereira[2] · Konstantin Nikolaou[1] · Stephan Clasen[1]

Abstract

Objectives Evaluation of the technical success, patient safety and technical effectiveness of magnetic resonance (MR)-guided microwave ablation of hepatic malignancies.

Methods Institutional review board approval and informed patient consent were obtained. Fifteen patients (59.8 years ± 9.5) with 18 hepatic malignancies (7 hepatocellular carcinomas, 11 metastases) underwent MR-guided microwave ablation using a 1.5-T MR system. Mean tumour size was 15.4 mm ± 7.7 (7-37 mm). Technical success and ablation zone diameters were assessed by post-ablative MR imaging. Technique effectiveness was assessed after 1 month. Complications were classified according to the Common Terminology Criteria for Adverse Events (CTCAE). Mean follow-up was 5.8 months ± 2.6 (1-10 months).

Results Technical success and technique effectiveness were achieved in all lesions. Lesions were treated using 2.5 ± 1.2 applicator positions. Mean energy and ablation duration per tumour were 37.6 kJ ± 21.7 (9-87 kJ) and 24.7 min ± 11.1 (7-49 min), respectively. Coagulation zone short- and long-axis diameters were 31.5 mm ± 10.5 (16-65 mm) and 52.7 mm ± 15.4 (27-94 mm), respectively. Two CTCAE-2-complications occurred (pneumothorax, pleural effusion). Seven patients developed new tumour manifestations in the untreated liver. Local tumour progression was not observed.

Conclusions Microwave ablation is feasible under near real-time MR guidance and provides effective treatment of hepatic malignancies in one session.

Key Points
• *Planning, applicator placement and therapy monitoring are possible without using contrast enhancement*
• *Energy transmission from the generator to the scanner room is safely possible*
• *MR-guided microwave ablation provides effective treatment of hepatic malignancies in one session*
• *Therapy monitoring is possible without applicator retraction from the ablation site*

✉ Rüdiger Hoffmann
  Ruediger.Hoffmann@med.uni-tuebingen.de

1   Department of Diagnostic and Interventional Radiology,
    Eberhard-Karls-University, Hoppe-Seyler-Strasse 3,
    72076 Tübingen, Germany

2   Department of Radiology, Minimally Invasive Therapies and
    Nuclear Medicine, SLK-Kliniken Heilbronn GmbH, Am
    Gesundbrunnen 20-26, 74078 Heilbronn, Germany

Introduction

Over the last two decades, percutaneous tumour ablation has become a promising treatment option for many patients with hepatic malignancies who are not able to undergo surgical resection due to comorbidity, limited hepatic function or unfavourable anatomic conditions [1, 2]. Radiofrequency (RF) ablation is the most common representative modality in the group of ablative therapies; however, studies have shown that tumour size over 3 cm and location close to large vessels are associated with an increased risk of local tumour recurrence [3, 4]. In this respect, microwave ablation has become an alternative to RF ablation, providing advantageous physical features. In comparison with RF ablation, microwave ablation enables higher intra-tumoural temperatures as it is

independent of increasing impedance, resulting in larger ablation zones in a shorter time, even with a single probe [5–7]. Furthermore, microwave ablation is less susceptible to the heat sink effect of larger vessels, as microwave energy is directly transmitted to a defined target volume. Development of the ablation zone with microwave ablation is therefore less dependent on thermal conductivity of the target tissue than RF ablation [8, 9]. In line with these advantageous technical properties, recent studies have shown lower local recurrence rates in microwave ablation of larger tumours in comparison to RF ablation [10].

Another key point of successful tumour ablation is precise therapy monitoring, which is based on reliable imaging of the tumour and the ablation zone. Ultrasound as a guidance modality is inexpensive, fast and widely accessible; however, evaluation of the ablation zone may be impaired by gas formation at the ablation zone and by the patient's physical condition [11, 12]. Computed tomography (CT) offers precise imaging; however, differentiation between ablation zone and residual tumour is only possible for a limited time after application of an intravenous contrast agent [13]. Using magnetic resonance (MR) imaging as a guidance modality in ablation procedures is currently limited to a small number of centres specialised in MR-guided interventions and therapies, although MR guidance offers several advantages, such as near real-time fluoroscopic imaging, higher sensitivity in depicting small parenchymal lesions, free selection of imaging planes, monitoring of thermal effects, and absence of ionising radiation [14, 15]. However, the limited acceptance of MR imaging as a guidance modality is mainly caused by the restricted availability of MR scanners suitable for interventional procedures, and higher operating costs combined with longer durations of MR-guided interventions [16, 17]. Hence, creation of large ablation zones in a shorter time with a single applicator is of particular interest, especially in combination with MR guidance.

The aim of this study was the evaluation of the technical success, patient safety and technical effectiveness of MR-guided microwave ablation of primary and secondary hepatic malignancies using a wide-bore 1.5-T MR system.

Materials and methods

Patients and lesions treated

Institutional review board approval and informed patient consent regarding the prospective analysis of the clinical data were obtained for this single-centre study. Hepatic tumour ablations are routinely conducted with MR-guided microwave ablation at our institution. Internal preconditions for ablative treatment are a maximum of three liver metastases or hepatocellular carcinoma (HCC) lesions and a maximum tumour

diameter of 5 cm. Further preconditions for MR-guided tumour ablation are an adequate coagulation status (platelet count >50,000/μL, Quick test >50 %) and absence of contraindications to MR imaging. Final decision for percutaneous tumour ablation was made by an interdisciplinary tumour board.

Between February and October 2015, 15 consecutive patients (12 men, 3 women) were treated with percutaneous microwave ablation for hepatic malignancies. All procedures were conducted under MR guidance as none of the patients had contraindications to MR imaging. Average patient age was 59.8 years ± 9.5 standard deviation (SD) (range, 44-77 years; median, 57). A total of 18 lesions were treated in 15 interventions; 6 patients were treated for 7 HCCs, 9 patients were treated for 11 hepatic metastases. The mean lesion size was 15.4 mm ± 7.7 (range, 7-37 mm; median, 12.5). One patient with HCC received platelet concentrate before the intervention to raise the platelet count above 50,000/μL. Two patients with HCC with a diameter above 3 cm were pre-treated with transarterial chemoembolisation 1 week before microwave ablation. Table 1 summarises the patients' characteristics.

Technical equipment

Ablations were performed with a tumour permittivity feedback control microwave ablation system tuned to the dielectric properties of hepatic tumours with a maximum antenna power of 36 W (Medwaves Avecure™ Microwave Generator; Medwaves, San Diego, CA, USA). Ablations were performed under temperature control mode: the pulsed output-power and microwave frequency (range, 902-928 MHz) were automatically adjusted by the generator, depending on the target tumour permittivity, to maintain an operator-selected ablation temperature measured using an integrated temperature sensor at the antenna tip. The ablations were performed using a single 16-G, MR-compatible microwave applicator with a shaft length of 16 cm and an active tip length of 4 cm [16-15-LH-35(MR); Medwaves] or 2 cm [16-15-LH-15(MR); Medwaves]. The pre-selected target temperature was 110 °C for the 2-cm active tip antenna and 120 °C for the 4-cm active tip antenna. The antenna was connected to the generator via a MR-compatible 2.4-m coaxial cable plus an additional 3.6-m extension coaxial cable, enabling positioning of the generator outside the scanner room. Connections were made through a cable tunnel. Interventions were conducted in a wide-bore 1.5-T system (Siemens MAGNETOM Espree; Siemens Healthcare, Erlangen, Germany) with a bore diameter of 70 cm. An RF-shielded liquid crystal display (LCD) monitor was installed next to the magnet for real-time monitoring. Patients' pulse rate and oxygen saturation were monitored using a MR-compatible patient monitor (Invivo 4500 MRI; Invivo Research INC, Orlando, USA).

Table 1 Patient and tumour characteristics

Patient no./ sex/age (years)	Tumour no.	Liver segment	Tumour entity	Maximal tumour diameter (mm)
1/F/49	1	VIII	Metastasis ovarian carcinoma	20
2/F/44	2.1	II	Metastasis CRC	11
	2.2	VII	Metastasis CRC	13
3/M/56	3	VIII	Metastasis melanoma	16
4/M/55	4	III	Metastasis CRC	16
5/M/49	5	VII	Metastasis CRC	8
6/M/68	6.1	IV	Metastasis CRC	10
	6.2	V	Metastasis CRC	7
7/F/57	7	VI	Metastasis CRC	12
8/M/56	8	VIII	Metastasis CRC	11
9/M/72	9	VII	HCC	14
10/M/54	15	IV	Metastasis melanoma	10
11/M/53	11.1	VII	HCC	11
	11.2	VIII	HCC	10
12/M/77	12	IV	HCC	19
13/M/73	13	VIII	HCC[a]	31[b]
14/M/68	14	VIII	HCC[a]	37[b]
15/M/60	10	VIII	HCC	22

HCC hepatocellular carcinoma, *CRC* colorectal carcinoma

[a] Pretreated with transarterial chemoembolisation 7 days prior to microwave ablation

[b] Tumour diameter before transarterial chemoembolisation

Patient treatment

The interventions were performed in the following steps: planning, targeting, therapy monitoring and control. The details of the sequences of each step are summarised in Table 2. Procedures were performed by either one of two radiologists with 6 and 9 years of experience in MR-guided interventions, respectively. Procedures were conducted under sedation analgesia ($n = 9$ patients; analgesia, 8-15 mg piritramide i.v.; sedation, 3-5 mg midazolam i.v.) or under general anaesthesia in cases of subcapsular tumour location ($n = 6$ patients). The patients were placed in a supine position and a capsule (Nifedipine AL 5; Aliud Pharma, Laichingen, Germany) was stuck to a potential applicator entry point as a marker for planning imaging. A six-channel body array coil and an additional one-channel loop coil were placed at the puncture site. A standardised planning MR protocol with unenhanced sequences was conducted to confirm the number, size and location of the target tumours and as baseline for therapy monitoring. Additional diffusion-weighted imaging (DWI) sequences and contrast-enhanced T1-weighted volumetric interpolated breath-hold examinations (VIBE) were optionally acquired in case of impaired tumour visualisation or suspicion of further hepatic tumour manifestation (Fig. 1). In one case, contrast enhanced dynamic liver imaging was acquired in the planning phase, after intravenous injection of 0.1 mmol gadobutrol (Gadovist; Bayer HealthCare, Leverkusen, Germany)

per kg body weight and in two cases after injection of 0.025 mmol per kg body weight of gadoxetate disodium (Primovist; Bayer HealthCare). Acquired three-dimensional (3D) T1-weighted VIBE was loaded to a dedicated interventional software (Interactive Front End, Work-In-Progress; Siemens Healthcare) enabling free slice angulation for planning of the applicator entry point and puncture path (Fig. 2). After labelling of the puncture site with a skin marker, disinfection, draping and local subcutaneous anaesthesia (Xylocaine 1 %; AstraZeneca, Wedel, Germany), a small skin incision was made at the entry point. The microwave antenna was inserted subcutaneously and sequences with T1 or T2 weighting (depending on the best tumour visualisation in the planning imaging) were acquired to confirm the correct position and angulation of the applicator. Targeting was conducted with a near real time, steady-state free precession fluoroscopic sequence (BEAT_IRTTT sequence), enabling continuous tracking of the antenna path in three angulations with a frame rate of 330 ms (Fig. 3). The applicator was advanced centrally into the target tumour until the centre of the active tip of the antenna coincided with the middle of the target tumour. The antenna was connected to the generator outside the scanner room via the extended MR-compatible coaxial cable and energy was applied according to the manufacturer's recommendations. After ablation, therapy monitoring sequences were acquired without having withdrawn the applicator. If the ablation zone which is demarcated as a T1 hyperintense area did

Table 2 Sequence details

Sequence	TE (ms)	TR (ms)	Slice thickness (mm)	Matrix	Flip angle	Bandwidth (Hz/pixel)
Planning						
T2 HASTE (coronal)	116	1100	6	256 × 205	120	488
T1 Flash 2D	4.1	211	6	256 × 150	70	140
T2 TSE	101	7500	6	320 × 186	150	300
T1 VIBE	1.3	3.6	2	256 × 140	10	454
Diffusion[a]	82	5020	5	128 × 100	90	1776
CE-dynamic T1 VIBE[a]	1.3	3.6	2	256 × 140	10	454
Targeting						
BEAT_IRTT (SSFP)	1.98	425	8	192 × 192	15	420
Therapy monitoring						
T1 Flash 2D	4.1	211	6	256 × 150	70	140
T1 VIBE	1.3	3.6	2	256 × 140	10	454
T2 TrueFISP	2.2	4.4	6	256 × 256	75	500
Control						
T2 HASTE (coronal)	116	1100	6	256 × 205	120	488
T2 TSE	101	7500	6	320 × 186	150	300
CE dynamic T1 VIBE	1.3	3.6	2	256 × 140	10	454

HASTE half acquisition single shot turbo spin echo, *Flash* fast low angle shot gradient echo, *TSE* turbo spin echo, *BEAT_IRTTT (balanced SSFP)* steady-state free precession (Siemens Corporate Research), *TrueFISP* True fast imaging with steady state precession, *Diffusion* echoplanar imaging with *b* values of 0, 400, 800 mm/s^2, *VIBE* volumetric interpolated breath-hold examination, *CE* contrast enhanced

[a] Optional

not cover the target tumour or residual tumour was assumed in T2-weighted images as hyperintense areas, ablation was continued with the same applicator position or after repositioning of the applicator under MR fluroscopic guidance (Fig. 4). If repeated therapy monitoring revealed a satisfactory result, the applicators were retracted and post-interventional control imaging was performed to evaluate technical success and to exclude complications such as active bleeding or cholestasis. Control sequences included contrast-enhanced dynamic T1-weighted VIBE after intravenous injection of 0.1 mmol gadobutrol per kg body weight (Gadovist).

Follow-up imaging

All patients underwent abdominal ultrasound 1 day post-ablation to exclude bleeding or cholestasis. Patients were discharged if ultrasound, blood count and their general condition were satisfactory. Follow-up scheme included liver MR imaging 4 weeks after ablation and every 3 months thereafter. Follow-up imaging was performed using a 1.5-T MR system (Siemens MAGNETOM Aera; Siemens Healthcare) with the following sequences: coronal T2-weighted half acquisition single shot turbo spin echo (HASTE), axial T2-weighted turbo spin echo sequence (TSE) with navigator technique, T1 TSE with breath-hold technique, echo planar imaging (EPI) for

DWI with *b* values of 0, 400 and 800 s/mm^2 and T1 VIBE dynamic liver examination after intravenous injection of 0.1 mmol gadobutrol (Gadovist) per kg body weight. Follow up imaging was assessed by a radiologist with 12 years of experience in abdominal MR imaging.

Data analysis

Technical success was assessed based on the contrast-enhanced control imaging after retraction of the microwave antenna. The procedure was considered to be technically successful if the ablation zone demarcated as a non-enhancing area in the late-enhancement images covered the pre-interventional tumour without evidence of residual tumour [18]. The short-axis and long-axis diameters of the ablation zone were evaluated using dedicated post-processing software (syngo.via; Siemens Healthcare). Technique effectiveness was defined as complete ablation at initial follow-up imaging 1 month after microwave ablation. Local tumour progression (LTP) was defined as detection of vital tumour adjacent to the ablation zone during follow-up [19]. Complications were based on the electronic patient records and classified in accordance with the Common Terminology Criteria for Adverse Events (CTCAE) of the National Cancer Institute [20]. Procedure-related information was collected from a
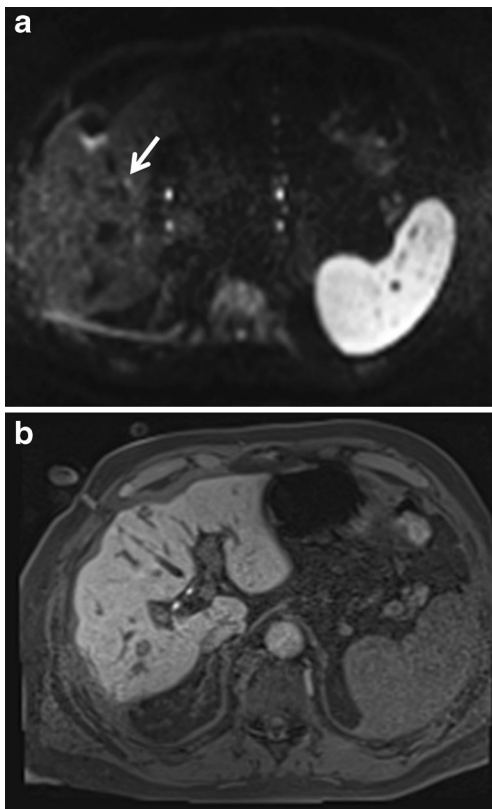
Fig. 1 A 68-year-old man, planned for microwave ablation of a single hepatic metastasis of a colon carcinoma (segment IV). Planning imaging included DWI (**a** b = 800 mm/s^2), which revealed a second, small hepatic lesion in segment V (*arrow*) which was considered suspicious as it was not detectable in former MR examinations. The suspicious lesion was targeted under orientation to neighbouring vessels as landmarks (**b** T1-weighted VIBE)

standardised form that was filled by the interventionist after treatment. Procedure duration was defined as time between acquisition of the initial localiser sequence and the final control sequence. Procedure duration was normalised with regard to the number of treated tumours.

Results

Technical success

Eighteen of 18 tumours were completely ablated, corresponding to a technical success rate of 100 %. The lesions were treated using 2.5 ± 1.2 applicator positions; 1-6 applicator positions were necessary for one target tumour (median, 2.0). Mean total duration of energy application was 24.7 ± 11.1 min (range, 7-49 min, median, 23.5 min). Mean energy applied was 37.6 ± 21.7 kJ per tumour (range, 9-87 kJ; median, 31.0 kJ). Six tumours were treated with a 2-cm active tip antenna; 12 tumours were treated with a 4-cm active tip antenna. Mean short-axis and long-axis diameters of the ablation zone were 31.5 mm ± 10.5 (range, 16-65 mm; median,

31.0 mm) and 52.7 mm ± 15.4 (range, 27-94 mm; median, 52.0 mm), respectively. Table 3 summarises the results with regard to the two different active tip lengths. Average duration of the interventions per tumour, including planning and control imaging, was 187 ± 64 min (range, 108-364 min; median, 174.5 min).

Technique effectiveness and local tumour progression

None of the ablation zones showed signs of incompleteness in the MR images after one month, resulting in a technique effectiveness of 100 %. Duration of follow-up ranged from 1-10 months (mean, 5.8 ± 2.7; median, 5.8); however, two patients had not reached the 4-month follow-up at the date of evaluation and manuscript preparation. During follow-up, no case of LTP was detected. However, seven patients developed new tumour manifestations in the untreated liver, of whom three were subsequently treated with chemotherapy, two with selective internal radiation therapy (SIRT), one with best supportive care and one patient was retreated with microwave ablation in a new hepatic HCC manifestation.

Complications and side effects

Two patients showed a T2 hyperintense zone with increased contrast enhancement along the extrahepatic applicator tract in the control imaging (Fig. 5). These observations occurred in tumours close to the hepatic capsule with a distance between the proximal end of the active antenna tip and the liver capsule of 12 and 15 mm, respectively. These alterations were distinctly regressive in the control MR imaging after 1 month and clinical evaluation did not show signs of skin burn. In one patient (no. 3), treated for a melanoma metastasis in segment VIII, a control chest X-ray was conducted 4 h after intervention, due to proximity of the antenna entry point to the pulmonary recesses. The chest X-ray revealed a pneumothorax that was treated with a chest tube (CTCAE Grade 2). Another patient (no.15) with liver cirrhosis, ascites and newly diagnosed partial portal vein thrombosis was treated for HCC in segment VIII as bridging therapy to liver transplantation. This patient developed a symptomatic pleural effusion after ablation treatment which was treated with thoracentesis (CTCAE Grade 2). Re-evaluation of the intra-procedural imaging revealed a probable antenna passage through the lateral pulmonary recesses during antenna positioning which probably caused shifting of ascites into the pleural space.

Discussion

An effective ablation system and a guidance modality enabling exact positioning and tumour targeting, as well as reliable assessment of the ablation zone, are essential for

Fig. 2 A 44-year-old woman, treated for two hepatic metastases of a colorectal carcinoma in segment II and VII. Unenhanced T1-weighted 3D VIBE was acquired for planning and loaded to dedicated interventional software (Interactive Front End, Work-In-Progress; Siemens Healthcare, Erlangen, Germany). A marker capsule was stuck to a potential entry point and depicts as a hyperintense spot. Based on the software, the applicator path was planned for targeting the hypointense tumour in segment VII. The display is subdivided into four viewports which show the path of the planed applicator tract in angulated axial (**a**), angulated sagittal (**b**) and in perpendicular angulation to the applicator tract at height of the target tumour (**c**, *arrow*). The determined slice angulations were applied for MR fluoroscopy for tumour targeting. The fourth viewport (**d**) shows a freely rotatable volume rendering technique (VRT) reconstruction of the planned applicator tract
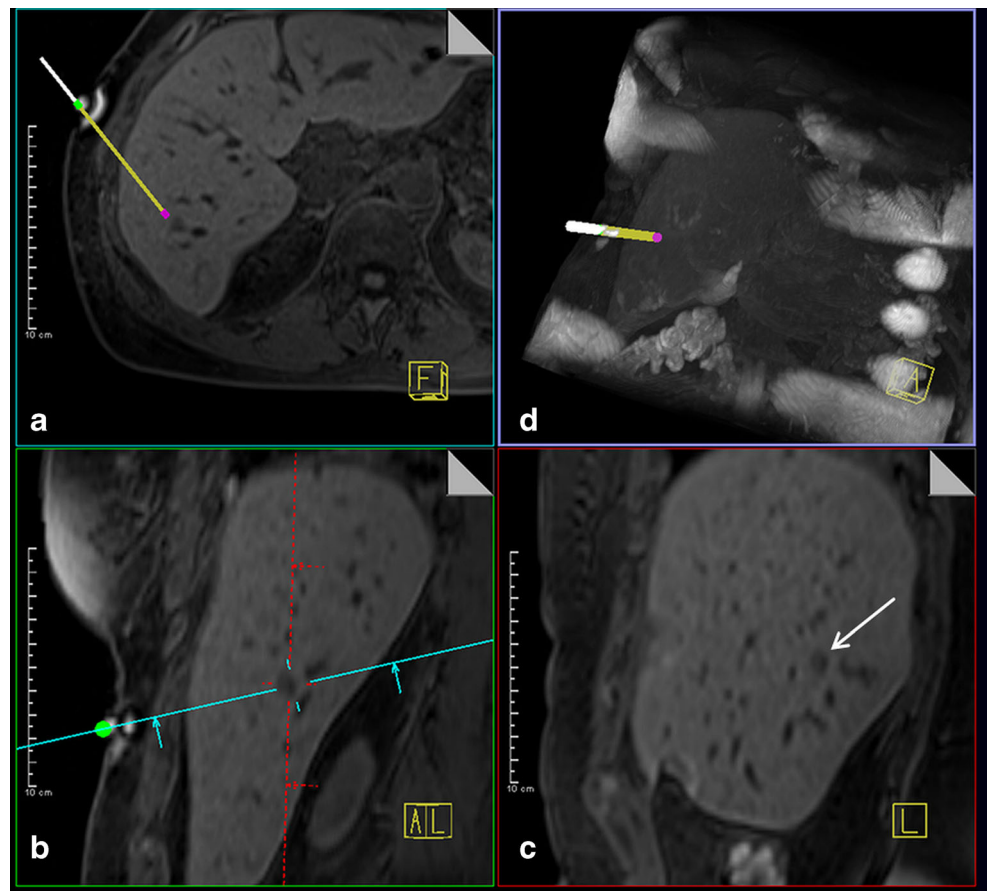
patient safety and therapy outcome in percutaneous hepatic tumour ablation. Several studies on MR guidance in RF ablation, laser interstitial thermal therapy (LITT) and high-intensity focused ultrasound (HIFU) have emphasised the value of this modality [21, 22]. Moreover, recent studies have proven high ablation performance of the latest generation of microwave ablation systems with shorter ablation durations, larger ablation zones and less susceptibility to heat sink effects in comparison to RF ablation [5, 23, 24]. Our study was conducted with a new, MR-compatible microwave ablation system with permittivity feedback control, enabling combination of both promising techniques: microwave technology for tumour ablation and MR imaging as a guidance modality. In our series, we reached technical success after all procedures and technique effectiveness was achieved in all treated hepatic tumours in the initial follow-up after 1 month. A potential factor for a high
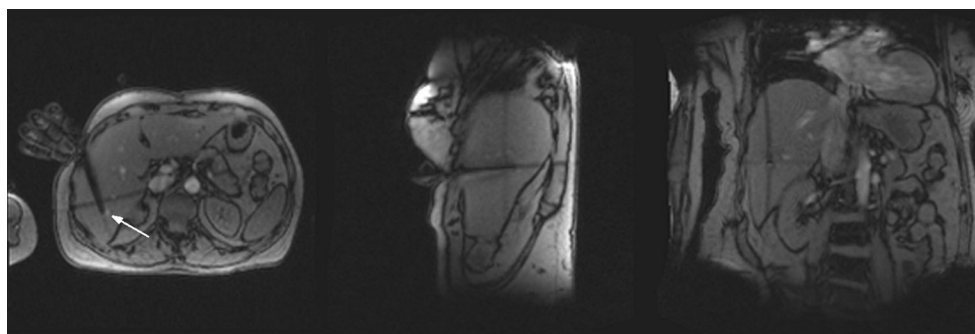

Fig. 3 A balanced SSFP (steady-state free precession) fluoroscopic sequence (BEAT_IRTTT) acquired during targeting of a hyperintense tumour in segment VII (*arrow*). Axial (**a**) and sagittal (**b**) slices are angulated on the microwave applicator; a coronal oblique slice (**c**) is angulated perpendicular to the applicator and positioned slightly ventral to the target tumour. An update rate of 330 ms enables near real time monitoring of the advancement of the hypointense artefact of the microwave applicator and the surrounding hyperintense hepatic vessels
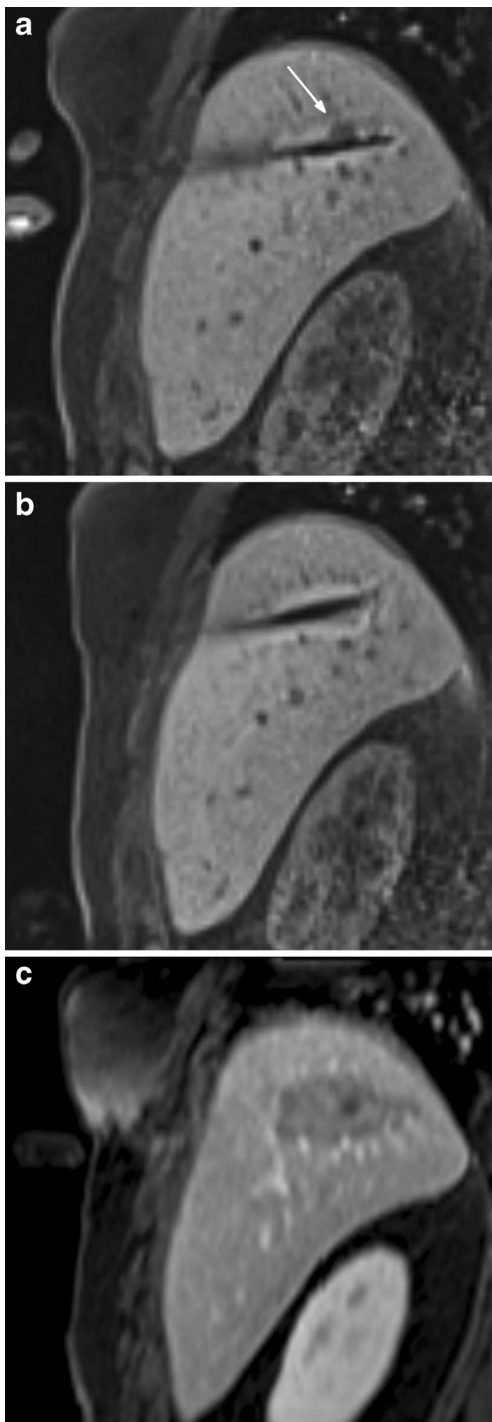
Fig. 4 Coronal T1-weighted VIBE therapy monitoring sequence shows the microwave applicator slightly eccentric and below a hypointense HCC in segment VII. After 15 min of ablation (**a**), the coagulation zone was depicted as a T1 hyperintense area with a missing safety margin at the apical part of the target tumour (*arrow*). The microwave applicator was repositioned there under MR-fluoroscopic guidance and ablation was continued for another 15 min. Coronal T1 VIBE therapy monitoring (**b**) then showed a sufficient coagulation area. Contrast-enhanced control sequences (T1 VIBE, portal venous phase) revealed the non-perfused ablation zone surrounding the former target tumour (**c**)

technique effectiveness rate is sufficient and reliable visualisation of the target tumour and the ablation zone. In this respect, Clasen et al. [25] stated a higher primary effectiveness rate after MR-guided hepatic RF ablation in comparison to procedures under CT guidance. Intravenous application of contrast agent is mostly necessary for tumour localisation and assessment of the ablation zone in ablation procedures under CT guidance [26]. However, the effect of contrast media is limited to a short time window after application and repetitive applications are restricted due the limited overall amount of applicable contrast media. In contrast, non-enhanced MR imaging offers a repeatable visualisation of tumour tissue, surrounding anatomy, and ablation zone. In our study the vast majority of planning, targeting and therapy monitoring could be conducted with non-enhanced MR imaging. Therefore, MR guidance is particularly advantageous in overlapping ablations as targeting and monitoring has to be repeated until complete coverage of the target tissue. In addition to conventional MR sequences, DWI was optionally acquired for planning imaging because of a high sensitivity for hepatic metastases [27]. DWI revealed a small but new and consequently suspicious second lesion in one patient planned for treatment of a single colorectal hepatic metastasis which was barely visible in the conventional sequences. Hence, this second lesion could be treated in the same session. In two cases, gadoxetic acid-enhanced MR imaging was required for planning. Besides a higher sensitivity for small hepatic malignancies compared with contrast-enhanced CT, gadoxetic acid-enhanced MR imaging has the best tumour visibility in the hepatobiliary phase after 20 min, whereas tumour visibility after application of CT contrast agent is restricted to a few minutes after application [28]. This point is of particular importance, as prolonged tumour visibility under gadoxetic acid enhancement enables tumour visibility until applicator placement [29]. Therapy monitoring with MR during RF ablation can be impaired by a prominent applicator artefact. T1-weighted sequences, in particular, have been reported to cause large artefacts of RF applicators with a diameter of 6-10 mm [30]. This can cause obscuration of the ablation zone or of surrounding critical structures and consequently makes retraction of the applicator from the tumour site necessary before acquisition of therapy monitoring sequences [31]. In our series, the MR artefact of the MW antenna did not obscure the borders of the ablation zone; thus, no retraction of the applicator was necessary for therapy monitoring. As a consequence, in cases where an inadequate ablation zone was suspected, the ablation could be continued without need for repositioning of the applicator. This is one of the beneficial features which may potentially decrease the duration of percutaneous tumour ablations; however, our procedure durations

Table 3 Procedure characteristics

Device	n	Max. tumour diameter (mm)	Positions	Ablation zone		Ablation duration (min)	Applied energy (kJ)	Total duration per tumour (min)
				SA (mm)	LA (mm)			
2-cm active tip	6	10.7 ± 2.7	2.3 ± 0.9	29.3 ± 8.7	37.2 ± 9.8	22.0 ± 13.5	27.5 ± 20.0	160 ± 34
4-cm active tip	12	17.8 ± 8.3	2.6 ± 1.3	32.6 ± 11.2	59.0 ± 12.1	26.0 ± 9.4	42.7 ± 20.7	201 ± 71
Overall	18	15.4 ± 7.7	2.5 ± 1.2	31.5 ± 10.6	52.7 ± 15.4	24.7 ± 11.1	37.6 ± 21.7	187 ± 64

SA short-axis diameter; *LA* long-axis diameter

did not show significant differences from reported MR-guided RF ablation, which were stated as 2-6 h [21]. A timesaving effect might eventually be observed in the interventions due to a learning curve; however, one time-critical point is the number of applicator positions. In the series presented here, an average of 2.5 applicator positions were necessary to treat one tumour, which prolongs the duration of the intervention, as applicator repositioning and further therapy monitoring is necessary. Therefore, further improvements of microwave-base

Fig. 5 A 49-year-old patient treated for hepatic metastasis of a colorectal carcinoma in segment VIII. Post-interventional T2-weighted TSE sequence (**a**) reveals a hyperintense, extrahepatic zone around the former applicator tract (*arrow*). This zone shows a slight contrast enhancement in the T1 VIBE portal venous phase (**b**). Distance between the proximal end of the applicator s active tip and the liver capsule measured 12 mm in this case

ablation procedures enabling larger ablation zones are desirable to increase the ratio of "one-position interventions" and consequently to obtain a significant reduction in overall procedure duration.

In two patients, control imaging revealed signal alterations of the extrahepatic applicator tract. Both cases occurred in ablations with a short distance between the antenna's active tip and the hepatic capsule. These changes are most likely to be explained by a warming of the extrahepatic antenna due to reduced heat convection in the peripheral liver tissue around the distal applicator shaft. Again, therapy monitoring by MR imaging may be advantageous to avoid critical heating of surrounding heat sensitive organs or extrahepatic tissue, especially in peripheral tumour locations.

There are some limitations to our study. First, our study cohort is relatively small and the follow-up period was too short for a reliable assessment of the local tumour recurrence rate. Consequently further studies with a longer follow-up period are necessary for evaluation of the outcome. Furthermore, we did not exclude pre-treated patients from this study, as these are part of our patient population in clinical routine. However, inclusion of pre-treated patients may influence treatment efficacy and safety. As in all other technical fields, there is continuous technical progression in microwave ablation techniques. At the end of the inclusion period of our study, the manufacturer launched a new, 14-G, MR-compatible microwave antenna. Further studies with revised ablation devices will have to evaluate if a reduction in procedure duration is achievable under maintenance of satisfactory ablation results. Another limitation is the underestimation of the ablation zone. Our measurements were based on the post-interventional MR imaging, showing the contracted ablation zone after treatment. This zone is smaller than the corresponding untreated tissue, leading to a underestimation of the originally ablated volume [32].

In conclusion, MR-guided microwave ablation provides effective treatment of primary and secondary hepatic malignancies in one session. MR imaging as a guidance modality enables planning, microwave applicator placement and therapy monitoring without the use of contrast enhancement in most cases. Retraction of the microwave applicator is not necessary for evaluation of the ablation zone, which may be one
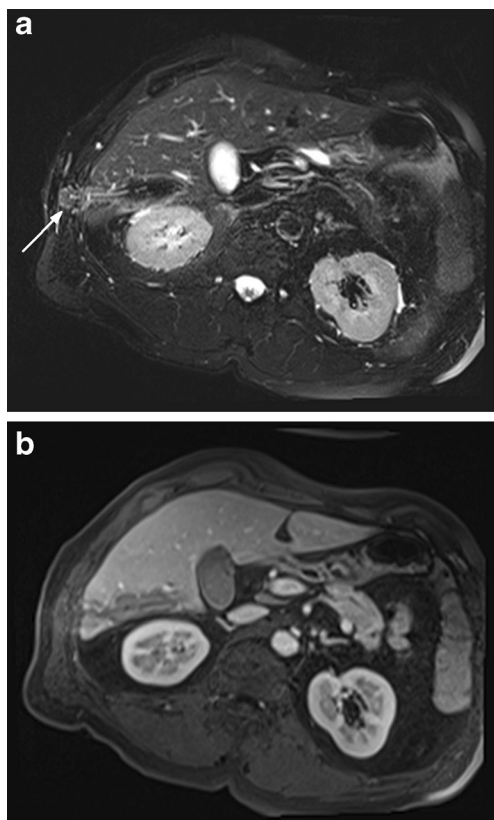
factor in reducing procedure duration. However, future studies are necessary to further evaluate the long-term outcome and the timesaving potential of this method.

References

1. Solbiati L, Ahmed M, Cova L, Ierace T, Brioschi M, Goldberg SN (2012) Small liver colorectal metastases treated with percutaneous radiofrequency ablation: local response rate and long-term survival with up to 10-year follow-up. Radiology 265: 958–968

2. Gillams A, Goldberg N, Ahmed M et al (2015) Thermal ablation of colorectal liver metastases: a position paper by an international panel of ablation experts, the interventional oncology sans frontieres meeting 2013. Eur Radiol 25:3438–3454

3. Frericks BB, Ritz JP, Albrecht T et al (2008) Influence of intrahepatic vessels on volume and shape of percutaneous thermal ablation zones: in vivo evaluation in a porcine model. Invest Radiol 43:211–218

4. Lee HY, Rhim H, Lee MW et al (2013) Early diffuse recurrence of hepatocellular carcinoma after percutaneous radiofrequency ablation: analysis of risk factors. Eur Radiol 23:190–197

5. Fan W, Li X, Zhang L, Jiang H, Zhang J (2012) Comparison of microwave ablation and multipolar radiofrequency ablation in vivo using two internally cooled probes. AJR Am J Roentgenol 198: W46–W50

6. Laeseke PF, Lee FT Jr, Sampson LA, van der Weide DW, Brace CL (2009) Microwave ablation versus radiofrequency ablation in the kidney: high-power triaxial antennas create larger ablation zones than similarly sized internally cooled electrodes. J Vasc Interv Radiol 20:1224–1229

7. Alexander ES, Wolf FJ, Machan JT et al (2015) Microwave ablation of focal hepatic malignancies regardless of size: a 9-year retrospective study of 64 patients. Eur J Radiol 84:1083–1090

8. Andreano A, Brace CL (2013) A comparison of direct heating during radiofrequency and microwave ablation in ex vivo liver. Cardiovasc Intervent Radiol 36:505–511

9. Huang S, Yu J, Liang P et al (2014) Percutaneous microwave ablation for hepatocellular carcinoma adjacent to large vessels: a long-term follow-up. Eur J Radiol 83:552–558

10. Chinnaratha MA, Chuang MA, Fraser RJ, Woodman RJ, Wigg AJ (2016) Percutaneous thermal ablation for primary hepatocellular carcinoma: a systematic review and meta-analysis. J Gastroenterol Hepatol 31:294–301

11. Leyendecker JR, Dodd GD 3rd, Halff GA et al (2002) Sonographically observed echogenic response during intraoperative radiofrequency ablation of cirrhotic livers: pathologic correlation. AJR Am J Roentgenol 178:1147–1151

12. Yu J, Liang P, Yu XL et al (2015) Local tumour progression after ultrasound-guided microwave ablation of liver malignancies: risk factors analysis of 2529 tumours. Eur Radiol 25: 1119–1126

13. Park MH, Rhim H, Kim YS, Choi D, Lim HK, Lee WJ (2008) Spectrum of CT findings after radiofrequency ablation of hepatic tumors. Radiographics 28:379–390

14. Rempp H, Loh H, Hoffmann R et al (2014) Liver lesion conspicuity during real-time MR-guided radiofrequency applicator placement using spoiled gradient echo and balanced steady-state free precession imaging. J Magn Reson Imaging 40: 432–439

15. Anzidei M, Napoli A, Sandolo F et al (2014) Magnetic resonance-guided focused ultrasound ablation in abdominal moving organs: a feasibility study in selected cases of pancreatic and liver cancer. Cardiovasc Intervent Radiol 37:1611–1617

16. Hoffmann R, Thomas C, Rempp H et al (2012) Performing MR-guided biopsies in clinical routine: factors that influence accuracy and procedure time. Eur Radiol 22:663–671

17. Maurer MH, Schreiter N, de Bucourt M et al (2013) Cost comparison of nerve root infiltration of the lumbar spine under MRI and CT guidance. Eur Radiol 23:1487–1494

18. Kierans AS, Elazzazi M, Braga L et al (2010) Thermoablative treatments for malignant liver lesions: 10-year experience of MRI appearances of treatment response. AJR Am J Roentgenol 194:523–529

19. Ahmed M, Solbiati L, Brace CL et al (2014) Image-guided tumor ablation: standardization of terminology and reporting criteria—a 10-year update. Radiology 273:241–260

20. Institute NC (June 14, 2010) Common Terminology Criteria for Adverse Events (CTCAE). Version 4.03. Available at: http://evs.nci.nih.gov/ftp1/CTCAE/CTCAE_4.03_2010-06-14_QuickReference_5x7.pdf. Accessed 16 January 2016

21. Rempp H, Waibel L, Hoffmann R, Claussen CD, Pereira PL, Clasen S (2012) MR-guided radiofrequency ablation using a wide-bore 1.5-T MR system: clinical results of 213 treated liver lesions. Eur Radiol 22:1972–1982

22. Mindjuk I, Trumm CG, Herzog P, Stahl R, Matzko M (2015) MRI predictors of clinical success in MR-guided focused ultrasound (MRgFUS) treatments of uterine fibroids: results from a single centre. Eur Radiol 25:1317–1328

23. Ringe KI, Lutat C, Rieder C, Schenk A, Wacker F, Raatschen HJ (2015) Experimental evaluation of the heat sink effect in hepatic microwave ablation. PLoS One 10: e0134301

24. Qian GJ, Wang N, Shen Q et al (2012) Efficacy of microwave versus radiofrequency ablation for treatment of small hepatocellular carcinoma: experimental and clinical studies. Eur Radiol 22:1983–1990

25. Clasen S, Rempp H, Hoffmann R, Graf H, Pereira PL, Claussen CD (2014) Image-guided radiofrequency ablation of hepatocellular carcinoma (HCC): is MR guidance more effective than CT guidance? Eur J Radiol 83:111–116

26. Kim YS, Rhim H, Lim HK, Choi D, Lee MW, Park MJ (2011) Coagulation necrosis induced by radiofrequency ablation in the liver: histopathologic and radiologic review of usual to extremely rare changes. Radiographics 31:377–390

27. Holzapfel K, Reiser-Erkan C, Fingerle AA et al (2011) Comparison of diffusion-weighted MR imaging and multidetector-row CT in the detection of liver metastases in patients operated for pancreatic cancer. Abdom Imaging 36:179–184

28. Kim HS, Choi D, Kim SH et al (2013) Changes in the signal- and contrast-to-noise ratios of hepatocellular carcinomas on gadoxetic acid-enhanced dynamic MR imaging. Eur J Radiol 82:62–68

29. Fischbach F, Lohfink K, Gaffke G et al (2013) Magnetic resonance-guided freehand radiofrequency ablation of malignant liver lesions: a new simplified and time-efficient approach using an interactive open magnetic resonance scan platform and hepatocyte-specific contrast agent. Invest Radiol 48:422–428

30. Rempp H, Clasen S, Pereira PL (2012) Image-based monitoring of magnetic resonance-guided thermoablative therapies for liver tumors. Cardiovasc Intervent Radiol 35:1281–1294

31. Aube C, Schmidt D, Brieger J et al (2004) Magnetic resonance imaging characteristics of six radiofrequency electrodes in a phantom study. J Vasc Interv Radiol 15:385–392

32. Brace CL, Diaz TA, Hinshaw JL, Lee FT Jr (2010) Tissue contraction caused by radiofrequency and microwave ablation: a laboratory study in liver and lung. J Vasc Interv Radiol 21: 1280–1286